
Article:
Alli, S, Figueiredo, CA, Golbourn, B et al. (11 more authors) (2018) Brainstem blood brain barrier disruption using focused ultrasound: A demonstration of feasibility and enhanced doxorubicin delivery. Journal of Controlled Release, 281. pp. 29-41. ISSN 0168-3659

https://doi.org/10.1016/j.jconrel.2018.05.005

Brainstem Blood Brain Barrier Disruption using Focused Ultrasound: A Demonstration of Feasibility and Enhanced Doxorubicin Delivery.

Saira Alli MBBS[a,f], Carlyn A. Figueiredo MSc*[a,b], Brian Golbourn MSc* [b], Nesrin Sabha[c], Megan Yijun Wu[b], Andrew Bondoc MSc [a], Amanda Luck[a], Daniel Coluccia[a], Colin Maslink[a], Christian Smith PhD[a], Heiko Wurdak PhD[f], Kullervo Hynynen PhD[d,e], Meaghan O'Reilly PhD[d] and James T. Rutka MD, PhD, FRCSC**[a,b,g]

[a]Division of Neurosurgery, the Arthur and Sonia Labatt Brain Tumour Research Centre; [b]the Division of Laboratory Medicine and Pathobiology, the Hospital for Sick Children; [c]Program for Genetics and Genome Biology, Hospital for Sick Children; [d]Physical Sciences Platform, Sunnybrook Research Institute, Department of Medical Biophysics, University of Toronto; [e]Institute of Biomaterials and Biomedical Engineering, University of Toronto; [f]the Leeds Institute of Cancer and Pathology and [g]Department of Surgery, University of Toronto.

Competing interests: KH is the founder of FUS Instruments, from which he receives non study related support. All other authors have no competing financial interests.

Total manuscript word count: 6131

---

*These two authors contributed equally to this work.

**To whom correspondence should be addressed c/o: Division of Neurosurgery, Suite 1503, The Hospital for Sick Children, 555 University Avenue, Toronto, Ontario, CANADA M5G 1X8
Phone: 416-813-6425; Fax: 416-813-4975; Email: james.rutka@sickkids.ca

Abstract

Magnetic Resonance Image-guided Focused Ultrasound (MRgFUS) has been used to achieve transient BBB opening without tissue injury. Delivery of a targeted ultrasonic wave causes an interaction between administered microbubbles and the capillary bed resulting in enhanced vessel permeability. The use of MRgFUS in the brainstem has not previously been shown but could provide value in the treatment of tumours such as Diffuse Intrinsic Pontine Glioma (DIPG) where the intact BBB has contributed to the limited success of chemotherapy. Our primary objective was to determine whether the use of MRgFUS in this eloquent brain region could be performed without histological injury and functional deficits. Our secondary objective was to select an effective chemotherapeutic against patient derived DIPG cell lines and demonstrate enhanced brainstem delivery when combined with MRgFUS in vivo.

Female Sprague Dawley rats were randomised to one of four groups: 1) Microbubble administration but no MRgFUS treatment; 2) MRgFUS only; 3) MRgFUS + microbubbles; and 4) MRgFUS + microbubbles + cisplatin. Physiological assessment was performed by monitoring of heart and respiratory rates. Motor function and co-ordination were evaluated by Rotarod and grip strength testing. Histological analysis for haemorrhage (H&E), neuronal nuclei (NeuN) and apoptosis (cleaved Caspase-3) was also performed. A drug screen of eight chemotherapy agents was conducted in three patient-derived DIPG cell lines (SU-DIPG IV, SU-DIPG XIII and SU-DIPG XVII). Doxorubicin was identified as an effective agent. NOD/SCID/GAMMA (NSG) mice were subsequently administered with 5mg/kg of intravenous doxorubicin at the time of one of the following: 1) Microbubbles but no MRgFUS; 2) MRgFUS only; 3) MRgFUS + microbubbles and 4) no intervention. Brain specimens were extracted at 2 hours and doxorubicin quantification was conducted using liquid chromatography mass spectrometry (LC/MS).

BBB opening was confirmed by contrast enhancement on T1-weighted MR imaging and positive Evans blue staining of the brainstem. Normal cardiorespiratory parameters were preserved. Grip strength and Rotarod testing demonstrating no decline in performance across all groups. Histological analysis showed no evidence of haemorrhage, neuronal loss or increased apoptosis.

Doxorubicin demonstrated cytotoxicity against all three cell lines and is known to have poor BBB permeability. Quantities measured in the brainstem of NSG mice were highest in the group receiving MRgFUS and microbubbles (431.5 ng/g). This was significantly higher than in mice who received no intervention (7.6 ng/g).

Our data demonstrates both the preservation of histological and functional integrity of the brainstem following MRgFUS for BBB opening and the ability to significantly enhance drug delivery to the region, giving promise to the treatment of brainstem-specific conditions.

Keywords: Focused Ultrasound, Brainstem, Feasibility, Drug Delivery

Introduction

The human brainstem is perhaps the most eloquent brain region housing crucial regulatory centres of wakefulness and cardiorespiratory control in addition to cranial nerve nuclei and neural tracts relaying motor and sensory information between the brain, spinal cord and cerebellum. Tumours arising in the region are therefore difficult to treat. Those with well demarcated borders can be surgically resected but despite intra-operative monitoring of these crucial functions, significant morbidity can arise [1]. The most commonly occurring brainstem tumour however, displays a diffuse growth pattern and is therefore not amenable to surgical resection. Diffuse Intrinsic Pontine Glioma (DIPG) results in a near 100% fatality rate within 2 years of diagnosis [2] and is the leading cause of brain tumour deaths in children [3].

Clinical trials assessing both single agent and combination chemotherapies have failed to improve the survival of patients with DIPG [4,5]. A key factor believed to be limiting the

efficacy of these agents is an intact blood brain barrier (BBB) [6]. As such, the current standard of care consists of focal radiation therapy to the pons, which provides a transient improvement in symptoms but limited survival benefit.

The increased availability of biopsy and post-mortem specimens has enabled molecular profiling of DIPG demonstrating characteristic molecular alterations including epigenetic dysregulation as a key driver of tumorigenesis. Following whole genome and exome sequencing of patient samples, it was identified that 70-84% of DIPGs harbour a point mutation in the histone variants H3.1 and H3.3 [7-9]. This somatic gain of function mutation results in a lysine 27 to methionine substitution (p.Lys27Met, K27M) and enhanced gene transcription [10]. In addition, the majority of H3K27M mutants are associated with aberrations within the TP53 pathway and/or growth factor pathways in brain development including ACVR1/ALK2, FGFR1, PI3KR1 and PDGFRA [11-14]. These findings have led to the advancement of pre-clinical models as well as new therapeutics. Rather promisingly, the histone deacetylase (HDAC) inhibitor, Panobinostat has demonstrated pre-clincial efficacy and is currently in Phase 1 trial (PBTC-047) [15].

These newer molecularly targeted therapies still face the challenge of achieving sufficient BBB penetration to result in clinically significant survival. MRI guided focused ultrasound (MRgFUS) provides a non-invasive means of focally disrupting the BBB. The technique uses low frequency ultrasound waves in combination with intravenously administered microbubbles (μBs) to transiently open the BBB without tissue injury [16-18]. When circulating μBs encounter focused ultrasound (FUS) energy, they expand and contract in a process known as stable cavitation, exerting a mechanical force on the blood vessel wall causing rearrangement of tight junction proteins and increased active transport [19,20]. This effect is transitory, lasting between 4-6 hours [21,22]. Although microbubbles are

commercially approved as ultrasound contrast agents, it is important to highlight that their use in conjunction with focused ultrasound for BBB disruption is currently experimental.

The integration of magnetic resonance image (MRI) guidance allows targeting of specific regions thereby preserving the integrity of the BBB elsewhere. MRgFUS has been shown to concentrate chemotherapeutics and macromolecules in targeted brain tissue as well as tumours with significant treatment effect [23-26]. Furthermore, the technique has been clinically translated with the design of a spherical, phased array, multi-element transducer helmet that enables ultrasound waves to penetrate the human calvarium [27], (ExAblate low frequency system, InSightec).

MRgFUS disruption of the BBB in the brainstem has not been studied to date. In this study, our primary objective was to determine the feasibility and safety of BBB disruption in the brainstem using MRgFUS in a rodent model. Our secondary objective was to identify an effective conventional chemotherapy agent against in vitro DIPG cell lines and to then determine the extent of enhanced brainstem delivery when combined with MRgFUS in vivo.

Materials and Methods

Animals

For experiments pertaining to the safety of MRgFUS in the brainstem, female Sprague Dawley rats (Jackson Laboratory) were used, weighing 150 – 250g at the start of each experiment. For experiments assessing Doxorubicin delivery to the brainstem, female NOD/SCID/GAMMA (NSG) mice (20 – 25g, Jackson Laboratory) were used. All animals were housed at constant temperature (23 ± 1°C) and relative humidity (60 ± 5%) with free access to food and water and a fixed 12-h light/dark cycle.

The use of animals and all animal procedures was approved by the Animal Care Committee at Sunnybrook Health Sciences Centre. All protocols used were in accordance with

the guidelines established by the Canadian Council on animal care and the Animals for Research Act of Ontario, Canada.

Magnetic Resonance guided Focused Ultrasound of the Brainstem:

Sprague Dawley Rats

Forty-two female Sprague Dawley rats (weight 150 – 250g) were anaesthetised using inhaled isofluorane anaesthesia in an animal chamber prior to repositioning in a nose-cone. Hair over the dorsal aspect of the skull was shaved and further removed with depilatory cream. A 22g angio-catheter was inserted into the tail vein. The animal was placed and secured in a supine position, on a mount designed for targeted focused ultrasound delivery. Registration of the animal's position within the mount was conducted with a 7T MRI scanner (BioSpin 7030; Bruker, Billerica, Mass). The exposed scalp was positioned on the water pack portion of the mount with ultrasound gel used between the 2 surfaces to achieve acoustic wave coupling. Initial T2 and T1 weighted axial and sagittal images were performed and used to set right and left sided brainstem targets. Following imaging and registration, the mount and attached animal were returned to the focused ultrasound system. The water pack portion of the mount was positioned to overlie a chamber of degassed, deionized water containing the transducer [28].

For physiological monitoring, an MRI compatible foot sensor of the MouseOx Plus physiological monitor (Starr Life Sciences Corp, Oakmont, USA) was attached to the left hind paw of the rat. Signal confirmation was achieved and physiological monitoring and recording of heart and respiratory rate was initiated. Duration of monitoring extended from at least 4 minutes prior to initial right sided brainstem sonication and completed at least 4 minutes after left sided brainstem sonication. The timing of interventions was documented so as to later cross reference with the monitoring data. Data extracted was plotted and graphed using Graphpad Prism version 7 (California, USA).

An in-house-built three-axis focused ultrasound system was used. Ultrasound was generated using a 1.68MHz spherically-focused transducer (radius of curvature = 60mm, external diameter = 75mm, focal number 0.8). The transducer was driven by a function generator (33220A; Agilent Technologies, Santa Clara, CA) and a radiofrequency amplifier (NP2519; NP Technology, Newbury Park, CA). Each transcranial sonication consisted of 10-millisecond bursts at a 1-Hz pulse repetition frequency for a total of 2 minutes. Microbubbles (μBs) (Definity® Lantheus Medical Imaging, Inc., N. Billerica, MA, U.S.A) were diluted 1:10 in normal saline and administered intravenously (0.02mL/kg) at the onset of sonication. Microbubble emissions were detected during sonication by a custom built polyvinylidene difluoride hydrophone [29] connected to a scope card located in the controlling PC. Pressure amplitude was incremented after each burst (starting pressure 0.25, pressure increments of 0.025) until sub or ultraharmonic emissions were detected in the fast fourier transform, (FFT) of the captured hydrophone signal by the PC. The remainder of the sonication proceeded at 50% of this threshold pressure amplitude. This sonication protocol has been devised to ensure effective and replicable BBB opening without tissue injury [30].

A region consisting of a 4-point overlapping grid was treated in the right side of the pons and then repeated on the left side of the pons (**Fig. 1A**). The same dose of μBs was injected at the onset of the left sided sonication. Hence, the total μB dose delivered was 2 x 20uLkg. It should be noted that this is twice the clinically advised maximum dose of Definity microbubbles as an ultrasound contrast agent. The two regions were sonicated at least five minutes apart to allow clearance of μBs from the initial injection (microbubble half-life ≈ 5-7 minutes in Sprague Dawley rats) [31] Rodents allocated to the μB control group received the same intravenous doses of μBs and gadolinium contrast but not the delivery of focused ultrasound. They were however positioned in the FUS mount for the same duration of time as the treated animals. Rats allocated to the "MRgFUS" control group did not receive the doses

of μBs but focused ultrasound and gadolinium contrast were administered at consistent time points as in the treated groups. Pre- and post-procedure imaging sequences were the same across all groups. Rats randomised to the "MRgFUS + μB + Cisplatin" group received an intravenous bolus dose of cisplatin (1.5 mg/kg) during the first (right sided) sonication delivered.

NSG Mice

Sixteen female NSG mice (20 – 25g) were anaesthetised and prepared for MRgFUS delivery as above. A smaller 26 G catheter was used for tail vein catheterisation and a single 4-point overlapping grid was treated in the centre of the pons. The smaller cross-sectional area of the brainstem in mice did not necessitate an 8-point treatment regime to achieve coverage. All mice were intravenously administered 5mg/kg of Doxorubicin (Cat. No. S1208, Selleckchem) at the time of MRgFUS delivery, immediately following the intravenous administration of microbubbles. Five mice were randomly allocated to each group. Groups were; 1) "No intervention" – mice received no focused ultrasound intervention. Mice were placed on the focused ultrasound device for the same period of time and administered gadolinium contrast at the same dose and time points as mice receiving interventions 2) "MRgFUS" – control group receiving focused ultrasound delivery without intravenously administered microbubbles, 3) μB – control group receiving μBs without focused ultrasound energy and 4) "MRgFUS + μB" – treatment group receiving both focused ultrasound energy and intravenously administered μBs.

Assessment of BBB Disruption:

Magnetic Resonance Imaging:

Contrast enhanced (0.1ml/kg Gadovist; Bayer HealthCare Pharmaceuticals, Inc. Leverkusen, Germany) T1 weighted imaging was used to assess BBB disruption after focused ultrasound delivery. The contrast agent was delivered after the left sided brainstem sonication in rats and at the time of the single brainstem sonication in mice. This was four minutes prior to imaging. Images were extracted using the MIPAV (Medical Image Processing, Analysis and Visualization) application.

Evans Blue administration:

A 4% Evans Blue dye was intravenously injected (4ml/kg) into a cohort of rats (n=5 for each group; "MRgFUS", "μB" and "MRgFUS + μB" and n = 4 for the "Control" group). following the post procedure contrast enhanced MR imaging. Control rats received no intervention. Animals were maintained under anaesthesia using intramuscularly injected ketamine (100mg/ml Narketan; Vetoquinol, Toronto, at a dose of 100mg/kg) and xylazine (20mg/ml Rompun; Sigma-Aldrich, Toronto, 10mg/kg dose). Animals were euthanised at one hour after Evans Blue administration. They were deeply anaesthetised and transcardially perfused with 4% paraformaldehyde. Sectioning through the level of the pons was performed and images were taken using a dissecting microscope (Olympus SZX16).

Assessment of Motor Function:

Rotarod Testing:

Rats were briefly pre-trained on an automated 4 lane rotarod unit (Rota Rod RS, Letica Scientific Instruments, Panlab Harvard Apparatus) initially on a fixed speed setting. An accelerating protocol was then used whereby rats were placed on a rod that accelerated smoothly from 4 to 40rpm over a period of 1 minute. The length of time that each animal was able to stay on the rod was recorded as the latency to fall, registered automatically by a trip switch under the floor of each rotating drum. Five successive recordings were taken for each rat (with 5-minute rest intervals between each trial) on five consecutive mornings one week

prior and one week post brainstem sonication. The rats were not labelled regarding their randomization group and thus the operator conducting post-procedure testing was blinded to the intervention.

Grip Strength Testing:

Rat forelimb grip strength was measured using an electronic digital force gauge grip-strength meter with accompanying grid fixture (Bioseb Instruments, Pinellas Park, Florida, USA). Rats were placed onto the grid, allowing forelimbs to take grip. Rats were drawn back in a straight line away from the sensor until they eventually released their grip. The peak force (g) exerted by the animal's grip was recorded. Eight trials were conducted (with 5-minute rest intervals between each trial), on three alternate days, one week prior to and one week post brainstem sonication. A single operator was used for all grip strength recordings to reduce operator variability and was also blinded to the intervention.

Histologic Analysis:

Rats randomised to the "early" histology group (n = 3 per group) were euthanised 4 hours following their allocated intervention. The "late" histology group (n = 6 per group) were euthanised on day 14 post intervention, allowing for post procedure grip strength and rotarod testing. These time points were chosen to maximise the potential of capturing apoptosis which could arise in either an acute or delayed fashion. Furthermore, assessment of neuronal number following MRgFUS has previously been measured at 8 days following intervention. [30]. A cohort (n = 5) of untreated rats were sacrificed to provide negative control tissue. Brains were extracted and stored in 10% neutral buffered formalin. Fixed tissues were dehydrated and embedded in paraffin. Brains were axially sectioned in three regions of the brainstem. Five µm thick axial sections were cut and mounted onto slides and deparaffinised using xylene and hydrated with decreasing concentrations of ethanol. Haematoxylin and eosin (H&E) staining was used to determine the histopathological features. H&E stained sections were independently

reviewed by a veterinary pathologist who was blinded to the sample labels. Tissues were immunostained for NeuN (Abcam,1:1000) and cleaved caspase 3 (cell signalling, 1:100) to evaluate neuronal integrity and apoptosis respectively. Sections were imaged using a 3D Histech Panoramic 250 slide scanner. Quantification of staining was performed using the Quantification Centre (QC) feature of the Panoramic Viewer software application (3DHistech, Budapest, Hungary) which uses a colorimetric algorithm to calculate the percentage of positive pixels over a designated tissue area, defined as relative mask area (rMA). A protocol was created in the "histology" sub-feature and the brainstem was outlined in each sample as the region of interest.

Drug Screening

Cell lines described here were obtained through a Material Transfer Agreement with the originating institution, Stanford University. Cell lines were validated by DNA fingerprinting using short tandem repeat analysis. Eight chemotherapy agents were selected from prior published in vitro efficacy in either DIPG or paediatric high-grade glioma cell lines [32].. The HP-300 Digital Drug Dispenser was used to enable automated and accurate dispensing of drugs in a 384 well format. For each compound, a twelve-point dose range, customised from previously published IC50 data **(Fig. 7A),** was dispensed in a scrambled format to reduce plating artefacts. Each DIPG cell line (SU-DIPG IV, SU-DIPG XIII and SU-DIPG XVII) was plated into a 384 well plate (containing the chemotherapy agents) using the Thermo Multidrop (ThermoFischer Scientific, Canada) at 4000 cells per well. Viability was assessed at day 5. Alamar Blue® Cell Viability Reagent (ThermoFischer Scientific, Canada) was added to each well, again using the Thermo Multidrop, and incubated for 3 hr. Optical absorbance values at 550nm-590nm from each well were measured using a plate reader (Spectra Max Gemini EM). Percent cell viability at each drug concentration was determined relative to vehicle control

(DMSO) and IC50 values were calculated in excel using the XLfit Plugin (IDBS) with the Boltzmann sigmoidal curve fitting algorithm. Three replications were conducted for each cell line.

Liquid Chromatography-Tandem Mass Spectrometry (LC/MS/MS)

NSG mice were anaesthetised two hours following intravenous Doxorubicin delivery using intramuscularly injected ketamine (100mg/ml Narketan; Vetoquinol, Toronto, at a dose of 100mg/kg) and xylazine (20mg/ml Rompun; Sigma-Aldrich, Toronto, 10mg/kg dose). Once deeply anaesthetised, mice were transcardially perfused with 0.9% sodium chloride solution for seven minutes and then euthanised. Brains were extracted and divided into the cerebrum, cerebellum and brainstem, placed in individually labelled cryotubes and snap frozen in liquid nitrogen. Samples were stored at -80° C until analysis was conducted.

Samples were analysed by LC/MS/MS at the Analytical Facility for Bioactive Molecules (The Hospital for Sick Children, Toronto, Canada). Sample preparation was carried out under reduced light conditions and cold temperature (4°C) using only plasticware. Working solutions of daunorucin (0.2 µg/mL) and doxorubicin standard curve (nine points prepared by serial dilutions, ranging from 5 to 2500 ng/mL) were prepared fresh from 0.1mg/mL stock solutions kept at -80°C.

Frozen samples were weighed and transferred into Precellys homogenization tubes containing ceramic beads (Bertin Technologies, Rockville, Washington DC). Extraction solvent consisting of 60% acetonitrile and 40% 0.05 M ammonium acetate, pH 3.50 (v/v) was added to achieve 10mg/mL and homogenised using a Precellys 24 high-throughput homogenizer (Bertin Technologies, Rockville, Washington DC) - two 20 second bursts at 5500 rpm with a 30 second pause. 100 µL of the homogenised suspension (corresponding to 10 mg tissue) was transferred into a set of 1.5 mL Eppendorf tubes. Ten µL of working daunorubicin

was added followed by 100 µL of extraction solvent. Samples were mixed by vortex, kept on ice for ten minutes and centrifuged at 20,000 g for fifteen minutes at 4°C. Supernatants were taken to dryness under N2 gas. Residues were reconstituted in 100 µL of MeOH/H2O (50/50) + 0.1% formic acid, centrifuged at 20,000 g for ten minutes at 4°C and transferred into 200 µL plastic inserts for LC/MS/MS analysis.

Doxorubicin and daunorubicin were measured by LC/MS/MS using a QTRAP 5500 triple-quadruple mass spectrometer (Sciex: Framingham, Massachusetts, USA) in positive electrospray ionization mode by MRM data acquisition with an Agilent 1200 HPLC (Agilent Technologies: Santa Clara, California, USA). Chromatography was performed by automated injection of 3 µL on a Kinetex XB C18 column, 50 x 3 mm, 2.6 µm particle size (Phenomenex, Torrance, CA). The HPLC flow was maintained at 600 µL/minute with a gradient consisting of: A= Water + 0.1% Formic Acid and B = Acetonitrile + 0.1% Formic Acid. Total run time was 5 minutes.

Quantification was performed on Analyst 1.6.1 software (ABSciex: Framingham, Massachusetts, USA) by plotting the sample peak area ratios (analyte peak area/internal standard peak area) of doxorubicin against a standard curve generated from various concentrations of doxorubicin from 0.01 ng to 10 ng, spiked with the same amount of daunorubicin used for the samples and extracted in the same conditions. The use of daunorubicin as an internal standard is due to its structural similarity to doxorubicin and therefore similar extraction recovery and chromatographic properties. [33,34].

Statistical Analysis

Sprague Dawley Rats

Rotarod and grip strength data were analysed using a two-way mixed multivariate analysis of variance (MANOVA) with Tukey's post hoc test. Histology data was compared

using a three-way MANOVA with Tukey's post-hoc test. Significance was deemed an alpha level of $P < 0.05$ (*) or $P < 0.01$(**) with a 95% confidence interval.

Physiological monitoring of heart and respiratory rate were analysed using a two-way multivariate mixed model analysis of variance.

NSG Mice

Doxorubicin quantities between treatments and across brain regions (cerebrum, brainstem and cerebellum) by two-way mixed ANOVA. Significance levels were either $P < 0.05$ (*), $P < 0.01$ (**) or $P < 0.001$(***) with a 95% confidence interval. A two-way mixed ANOVA was used to compare doxorubicin quantities across brain regions.

Results

MRgFUS Parameters for BBB Disruption:

The average peak pressure amplitude reached across all sonications performed in rats was estimated to be 1.1 +/- 0.3 MPa and in mice was 0.71 +/- 0.15 MPa. The in situ pressures were estimated assuming a 55% transmission through the skull bone [35] and attenuation of 5 Np/m/MHz [18]through 5 mm of brain tissue. The assumed transmission of 55% through the skull bone at this frequency may result in an over-estimation of the true in situ pressures as this figure was obtained from measurements recorded through a more rostral portion of rat parietal bone [35]. The more posterior trajectory of ultrasound in our study, through a caudal portion of the skull with both an increased degree of curvature and thickness, would be expected to result in a higher insertion loss.

Confirmation of brainstem BBB opening:

Sprague Dawley rats

Two methods were used to confirm BBB disruption in the brainstem, namely focal gadolinium (Gad) enhancement on post procedure T1-weighted MR imaging **(Fig. 1)** and Evans Blue staining of gross histological specimens **(Fig. 2).** Immediately following sonication, only rats which received concurrent intravenous injection of µBs ("MRgFUS + µB" and "MRgFUS + µB + Cis") clearly showed localised Gad enhancement in the brainstem, indicating BBB disruption.

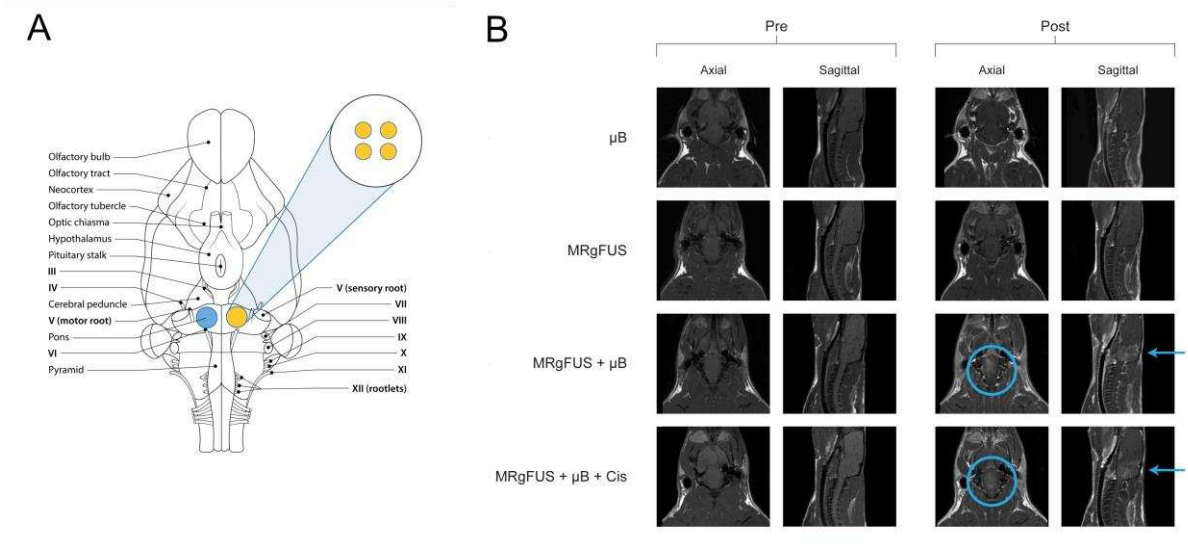

Figure 1: Brainstem sonication schema used in Sprague Dawley rats. (Colour Figure)

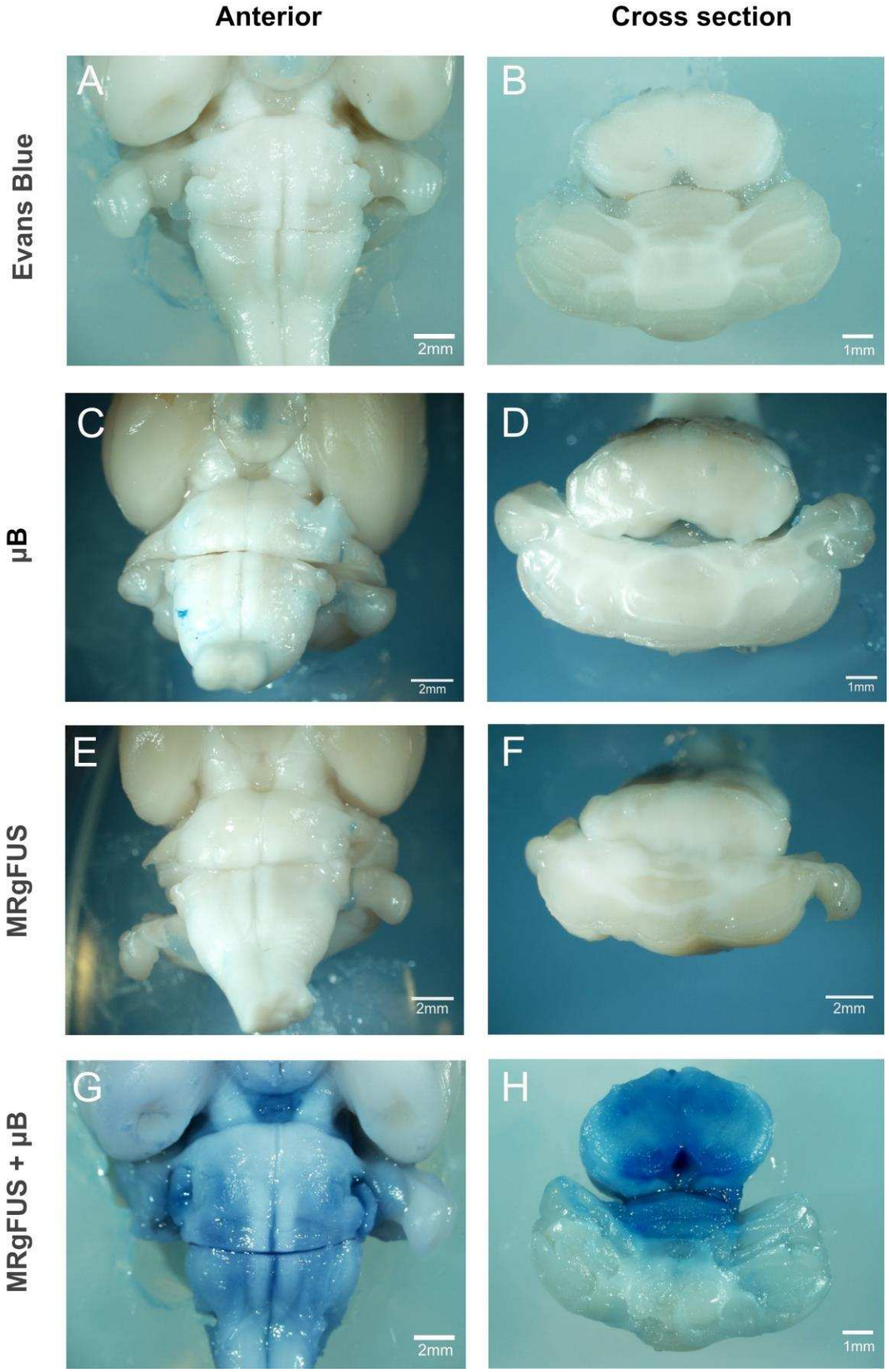

Figure 2: Evans Blue staining of rodent brainstem confirming BBB opening. (Colour

Figure)

To further confirm our MRI observations, intravenous Evans Blue was delivered following sonication to demonstrate the extent of BBB disruption histologically. Blue staining was observed on the ventral surface of the brainstem, in and around the region of the pons **(Fig. 2G)**. On sectioning through the brainstem at the level of the pons, blue staining of both the brainstem and a portion of the ventral cerebellum was evident **(Fig. 2H)**. The presence of dye in the brainstem was again only seen in the "MRgFUS + μB" group (the "MRgFUS + μB + Cis" group was not tested) and not in either the "MRgFUS" , "μB" or "control" groups **(Fig. 2A-F)**.

NSG Mice

Focal gadolinium enhancement on post-procedure T1 weighted imaging was used to confirm BBB disruption in NSG mice administered doxorubicin **(Supplementary Fig. 3).** As above, only mice in the "MRgFUS + μB" cohort demonstrated brainstem gadolinium enhancement **(Supplementary Fig. 3B)** indicating successful BBB permeability in the region.

Physiological monitoring of heart and respiratory rate during brainstem focused ultrasound delivery:

Grey matter nuclei contained within the brainstem include the cardiovascular and medullary rhythmicity centres which together control the heart rate, blood pressure and respiratory rate. As such, tissue injury to this region has the potential to affect these vital functions. Once under anaesthesia, rats were recorded for 4 minutes to determine baseline vital signs and ensure stable signal detection. Monitoring was continued throughout MRgFUS and for a further 4 minutes after. The normal heart rate in rats varies from 250 - 450 beats per minute with a respiratory rate up to 85 beats per minute. Although variability and fluctuations are seen in both parameters, these were not concurrent with periods of focused ultrasound

delivery (**Fig. 3** - pink bars) but rather occurred consistently throughout the period of monitoring. Statistical comparison was made of the mean heart rate and respiratory rate during and after MRgFUS delivery to that of baseline before intervention recordings and no significant difference was found (**Fig. 4**) Both parameters remained stable throughout the monitoring period with no persistent fluctuations from baseline or abrupt cessation of parameters. This was true for all animals across the different treatment groups **(Fig. 3 & 4)**.

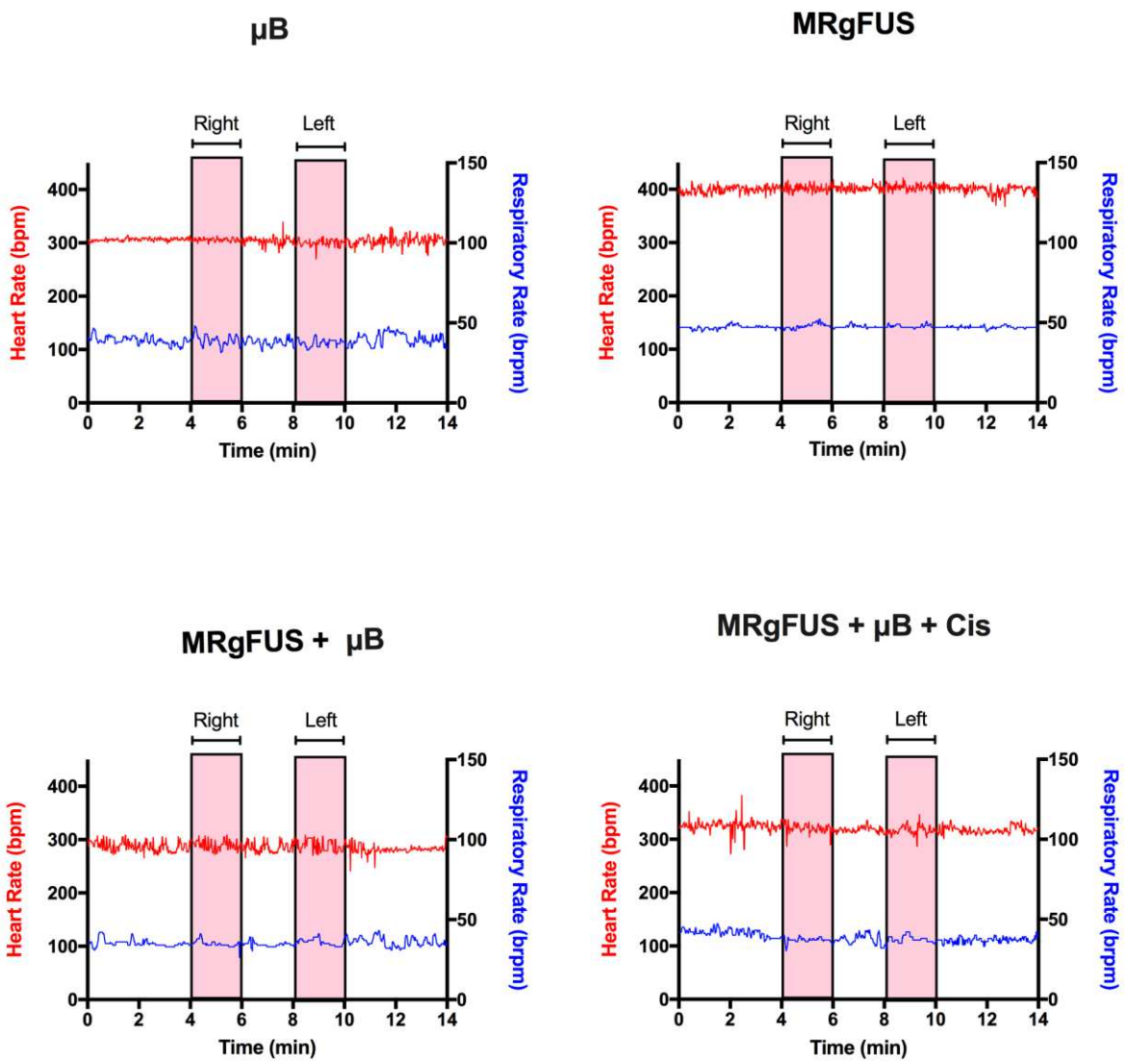

Figure 3: Physiological monitoring of heart and respiratory rate. (Colour Figure)

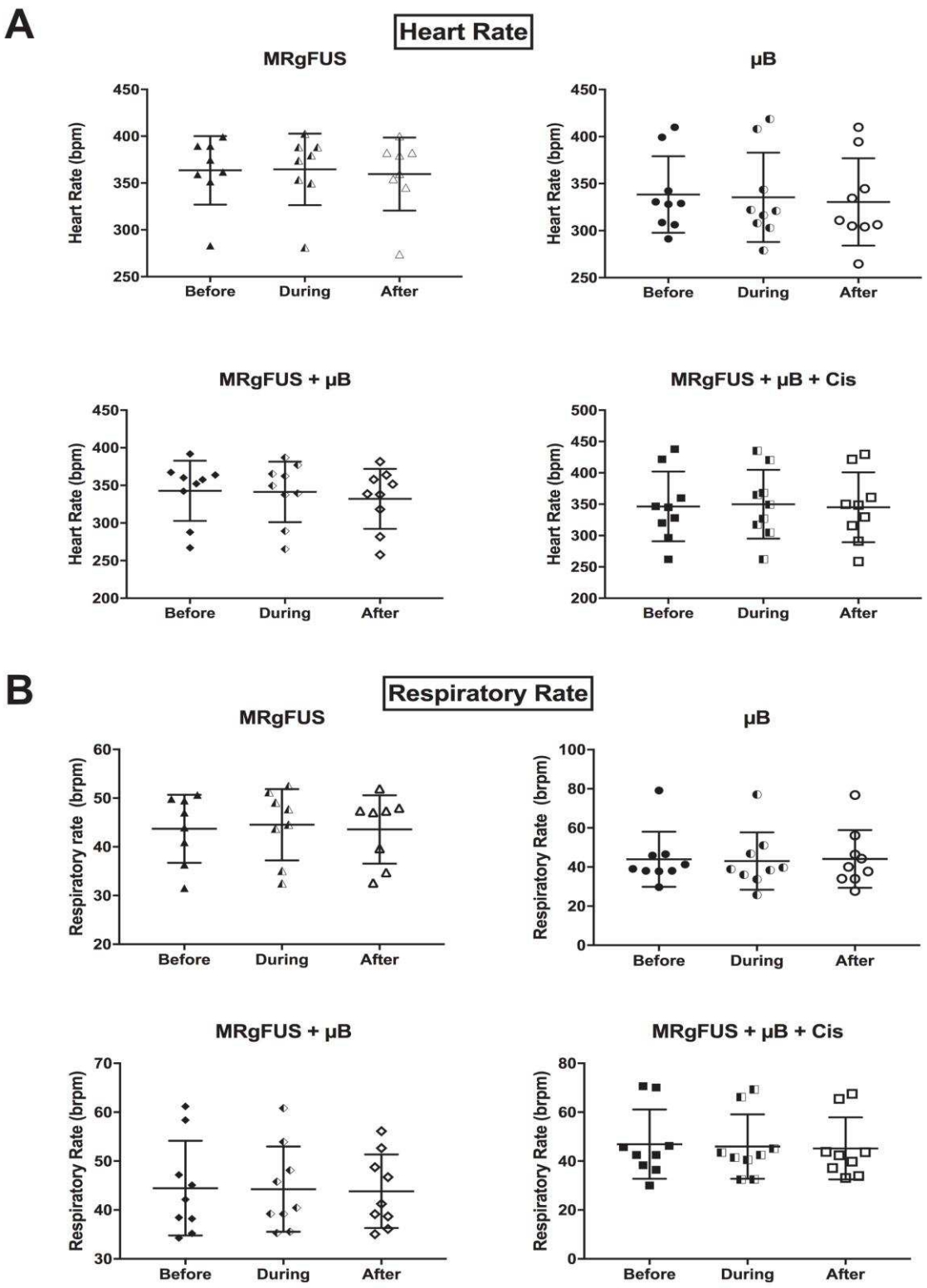

Figure 4: Comparison of (A) mean heart rate and (B) respiratory rate recordings of rats before, during and after the specified procedures.

Motor control and coordination following focused ultrasound delivery to the brainstem:

Both rotarod and grip strength data were compared pre- and post-MRgFUS delivery to the rat brainstem **(Fig. 5).** Comparison of post procedure performance with pre-procedure untreated performance provided an internal negative control. No statistically significant differences were identified in rotarod performance when comparing performance between groups. However, animals within each group demonstrated improved performance on post-procedure testing which may be attributed to the expected improvement in performance by animals with repeated measurements. **(Fig. 5A).** These findings were also found in grip strength testing **(Fig. 5B).**

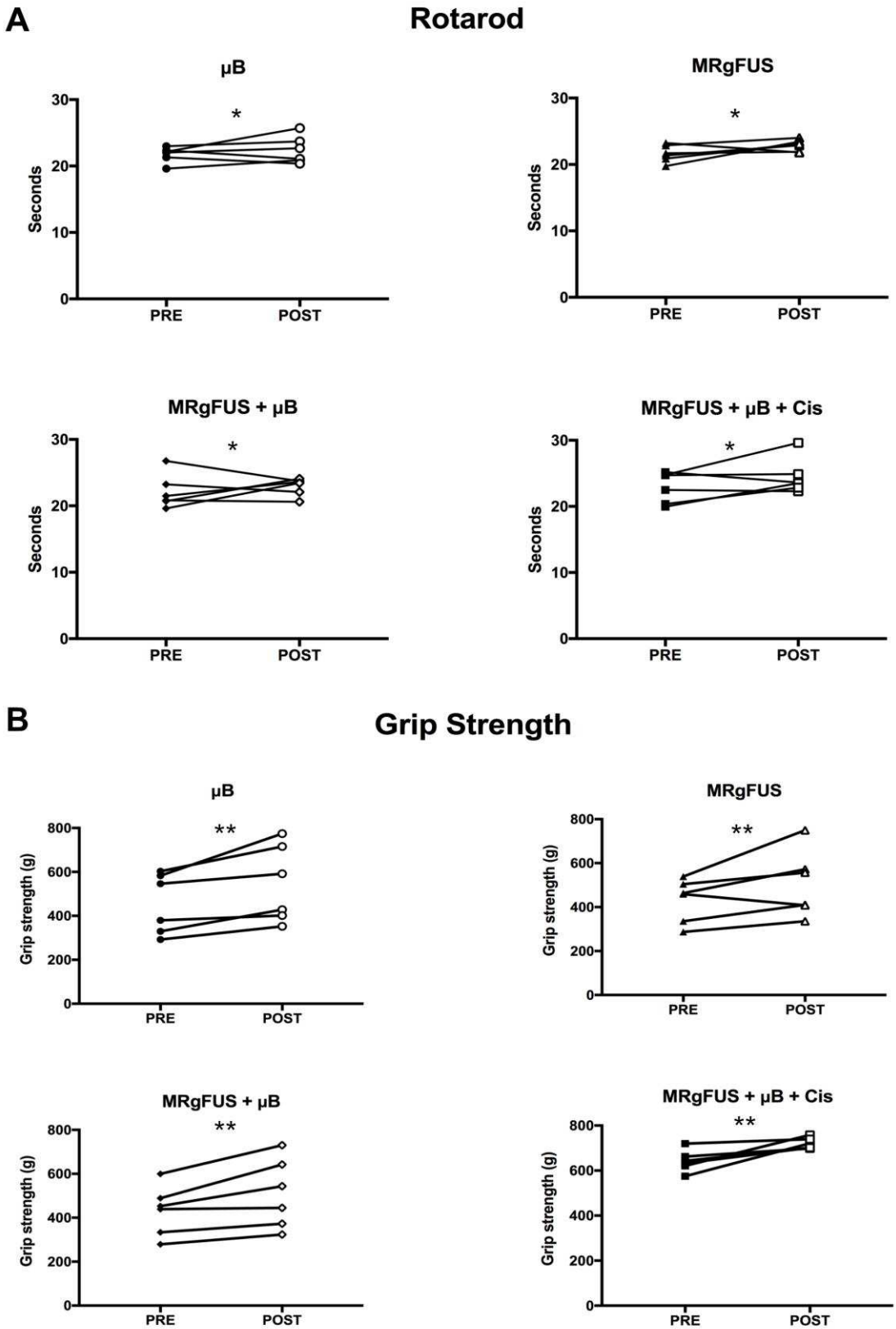

Figure 5: Comparison of rotarod and grip strength performance pre-and post-procedure.

Histological assessment of brainstem tissue:

Three levels of the rodent brainstem were assessed **(Fig. 6A)**. Sections were stained with H&E for cell morphology, Caspase-3 for apoptosis and NeuN for neuronal number. These parameters were chosen as focused ultrasound could potentially cause tissue damage in the form of haemorrhage and tissue vacuolation, increased apoptosis and neuronal loss [30,36]. At both early (4 hours) and late (14 day) time points, H&E stained sections did not show evidence of tissue damage or haemorrhage in any of our groups when compared with untreated controls **(Fig. 6B)**. This was independently verified by a veterinary pathologist who was blinded to the sample groupings. In addition, we did not note any significant differences in positive caspase 3 for any groups compared to untreated controls **(Fig. 7A & Supplementary Fig. 1)**. Similarly, there were no changes in neuronal number between groups, at all levels of the brainstem **(Fig. 7B & Supplementary Fig. 2)**.

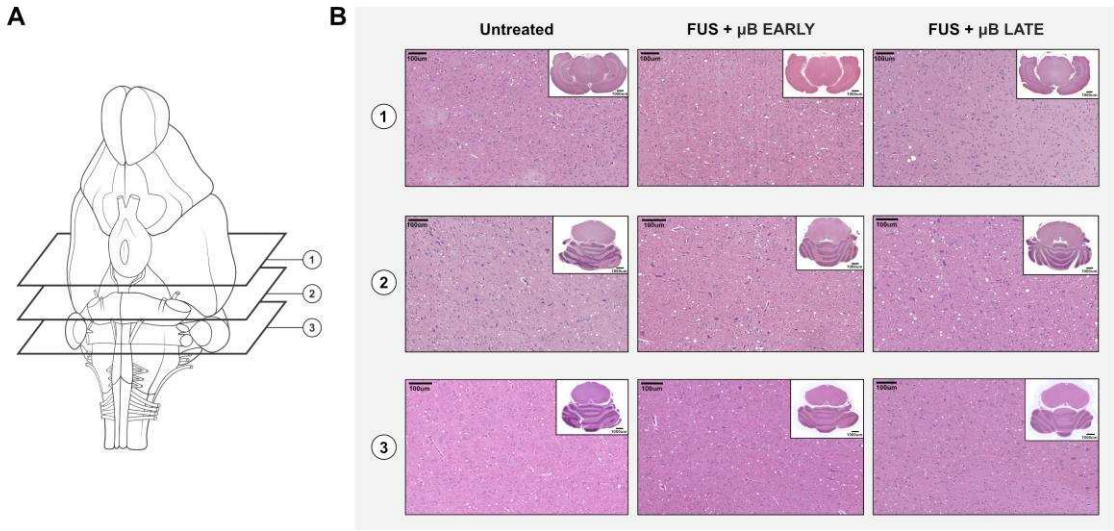

Figure 6: Hematoxylin and eosin (H&E) staining of brainstem sections. (Colour Figure)

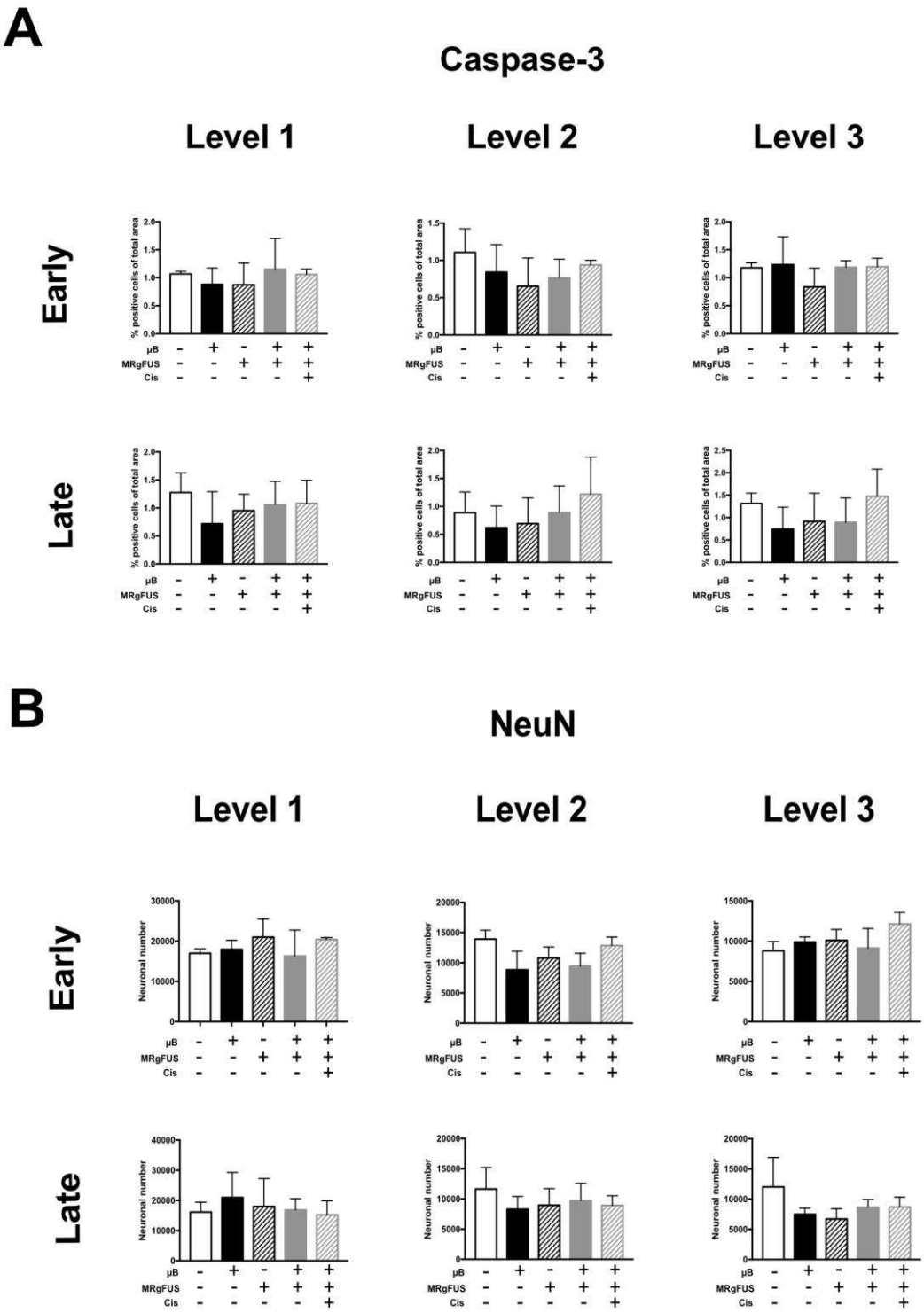

Figure 7: Quantification of Caspase 3 and NeuN staining of brainstem samples.

DIPG Drug Screen

We conducted a small screen of eight conventionally used chemotherapy agents in three patient-derived DIPG cell lines. Three agents; Etoposide, Doxorubicin and Mitoxantrone demonstrated significant toxicity across all three cell lines with correspondingly low IC_{50} values (mean values of 421nM, 49nM and 50nM respectively) **(Fig. 8B)**. Carboplatin, BCNU and Melphalan also demonstrated toxicity, but were less effective, requiring higher drug concentrations. In contrast, both Temozolamide and Cisplatin demonstrated little to no toxicity in these cell lines. Twelve-point dose escalation curves for Doxorubicin and Temozolamide can be seen in **Figure. 8C.**

A

Drug	Dose Range (uM)	
	Min	Max
Temozolamide	0.0488	200
Etoposide	0.488	200
Carboplatin	0.0488	100
Doxorubicin	0.0065	10
BCNU	0.0325	100
Melphalan	0.00325	50
Mitoxantrone	0.000325	5
Cisplatin	0.00325	50

B

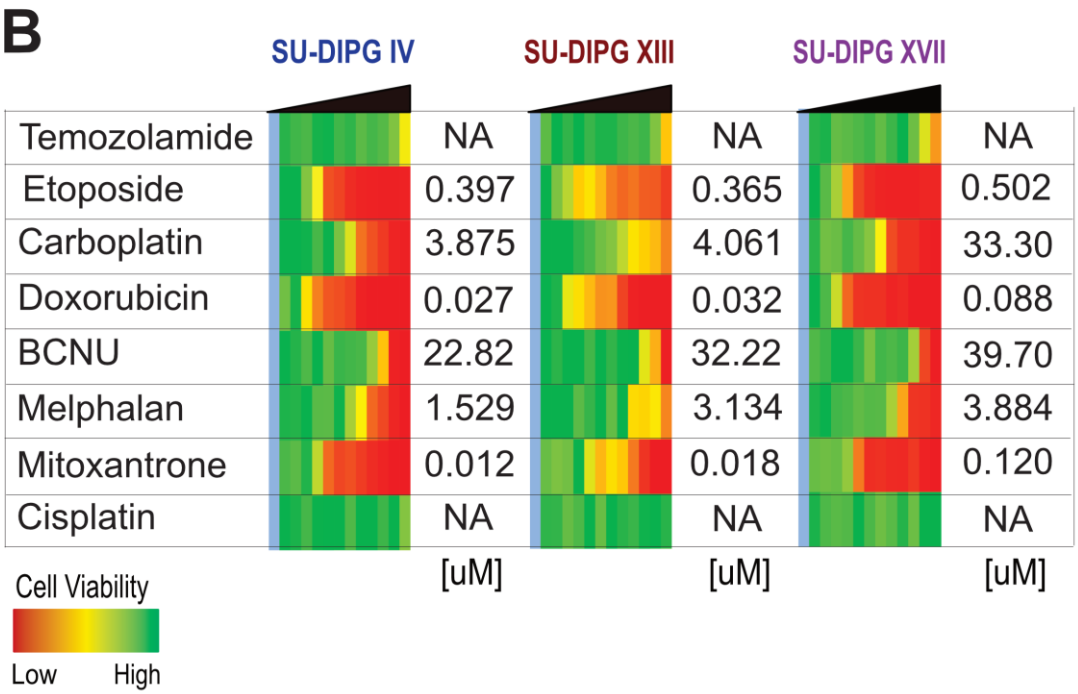

C

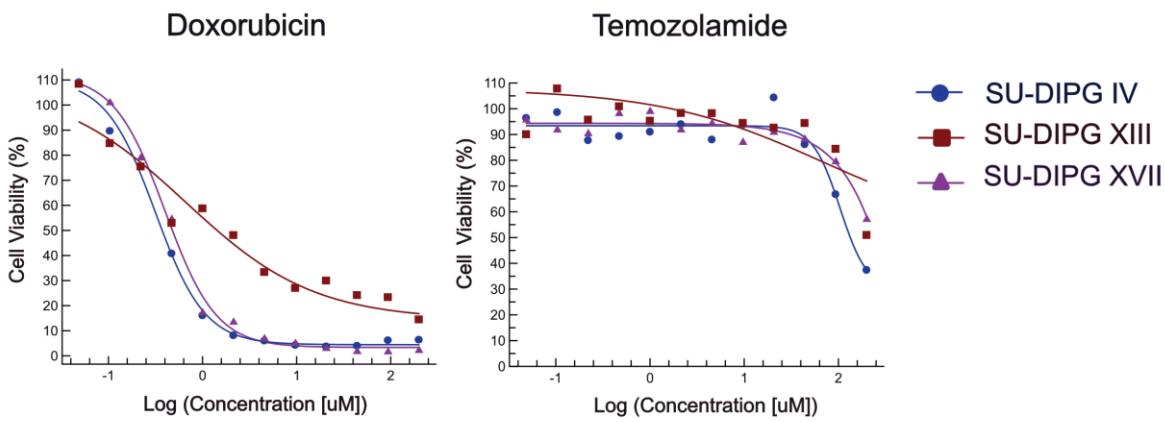

Figure 8: DIPG Drug Screen. (Colour Figure)

BBB disruption using MRgFUS enhances brainstem Doxorubicin uptake

Following its in vitro efficacy and with poor BBB permeability, Doxorubicin was selected as the chemotherapeutic agent with which to assess brainstem uptake when combined with focused ultrasound treatment **(Fig. 9).** The poor BBB permeability of Doxorubicin was confirmed in mice randomised to the "no intervention" group who received a 5mg/kg intravenous dose of Doxorubicin and who were subsequently found to have a mean brainstem value of 7.6ng/g at two hours. Similarly, low values of 18.7 ng/g and 12.31 ng/g were recorded in control groups receiving intravenous doxorubicin with either focused ultrasound energy alone (MRgFUS) or μBs alone. Successful BBB opening with MRgFUS and μB in combination with IV doxorubicin however, resulted in a significantly higher brainstem doxorubicin level of 431.5 ng/g. This is more than a 50-fold increase compared to the "no intervention" cohort and corresponds to a doxorubicin concentration of 824.2 nM (using a brain density of 1.04 g/mL [37]). This far exceeds the mean IC_{50} value of 49 nM of Doxorubicin recorded in our cell lines.

Furthermore, MRgFUS + μB + Doxorubicin treated mice showed significantly higher uptake in the brainstem alone as compared to the cerebrum and cerebellum ($p<0.001$). This is attributed to the focal disruption of the BBB in the brainstem using MR image guidance.

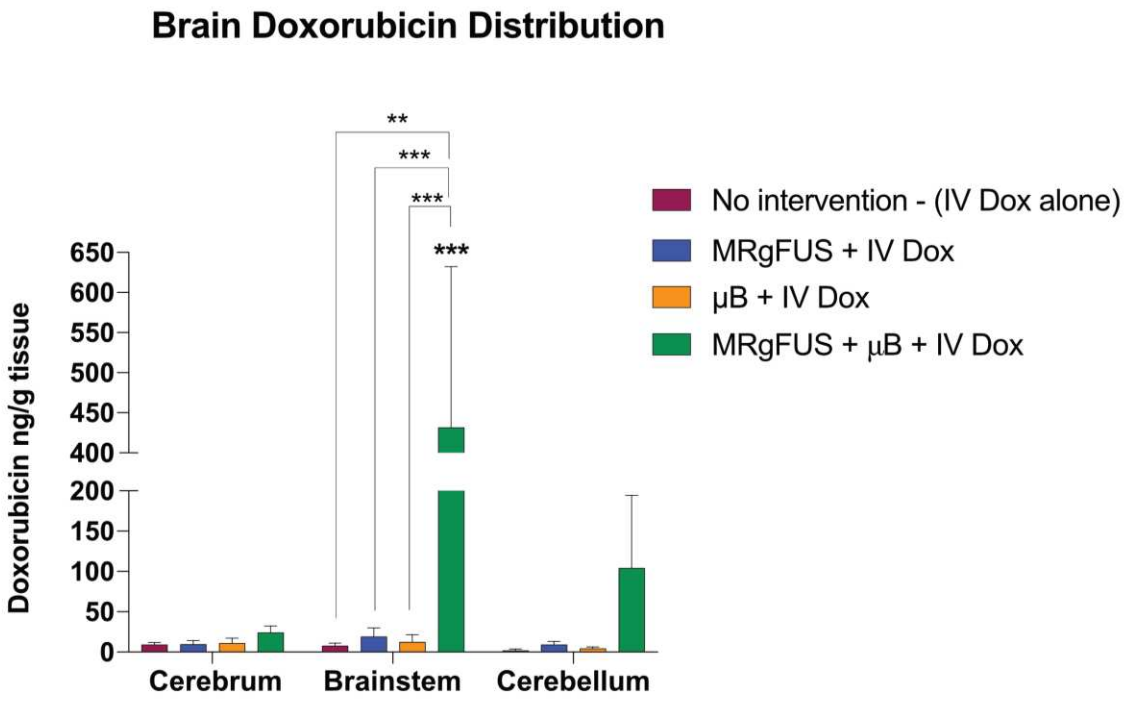

Figure 9: Brain Doxorubicin Distribution. (Colour Figure)

Discussion:

In this study, we have demonstrated effective BBB disruption in the rodent brainstem without evidence of tissue injury or functional motor deficit. By using a 4-point sonication grid in each half of the pons, we were able to achieve diffuse BBB opening in the region, confirmed by both gadolinium contrast enhancement on T1 weighted imaging and Evans Blue staining of the tissue. Following BBB disruption, there were no statistically significant alterations in critical cardiorespiratory vital signs. In addition, evaluation of motor pathways and cerebellar function revealed no decline in function as measured by retained grip strength and rotarod performance. Histological analysis of the sonicated regions of the brainstem at both early (4 hours) and late (14 day) time points revealed preserved brainstem architecture and neuronal numbers without activation of caspase 3 activity. BBB disruption and the administration of the

chemotherapeutic agent, cisplatin (1.5 mg/kg), was well tolerated without evidence of physiological brainstem dysfunction.

Further to this, we conducted a drug screen of existing chemotherapy agents which identified doxorubicin as an effective agent against patient derived DIPG cell lines. Doxorubicin is known to have poor BBB permeability [38,39] but when combined with MRgFUS BBB disruption, we were able to show highly effective passage of the drug into the brainstem. Importantly, the concentration reached in brainstem tissue far exceeded the in vitro IC_{50} concentration. The targeted brainstem BBB penetration also resulted in focally enhanced doxorubicin uptake to the region with limited uptake in other brain regions. Taken together, our data suggest that MRgFUS can be used to safely target the pons in an experimental model system and can significantly enhance drug delivery to the region. This technique may be a novel and exciting strategy to treat brainstem-specific disorders, such as DIPG.

To date, all chemotherapy trials for DIPG have failed to show improvements in overall survival. While treatment failures may relate to the selection of non-targeted drugs for DIPG or intrinsic tumour cell resistance mechanisms, another reason for failures may be the difficulty associated with achieving sufficient intra-tumoral doses within the brainstem [40]. The eloquent location of tumour in the brainstem and preservation of the BBB favour methods of drug delivery that are both non-invasive and low risk. Although efforts should be made to improve our understanding of the chemosensitivity of DIPG tumour cells, focal disruption of the BBB in a transient manner would ensure adequate delivery of appropriately selected drugs. As has been demonstrated in previous studies in the supratentorial compartment in human trials, MRgFUS allows for non-invasive, focal, reversible and repetitive BBB disruption [41].

Convection enhanced delivery (CED) is another technique that has been employed to improve the delivery of chemotherapeutics to the brainstem (see NCT01502917). The technique is currently not clinically approved but promising recent developments in the field

include the successful completion of a phase 1 trial in patients with DIPG [42] and FDA approval of a multi-port catheter. However, no drugs are currently approved for direct delivery into the brain parenchyma. CED is invasive, requiring the insertion of stereotactically guided catheters directly into the brainstem. As described, CED has some limitations: Only small volumes (< 3 mls) can be administrated safely; and only low infusion rates are tolerated [43]. In addition, with CED, drug reflux along the proximal catheter [44] and the limited extracellular space in the brainstem [43] hinder drug distribution, necessitating the use of multiple catheters [45]. As such, currently described methods of CED are best suited to short term drug delivery [44].

There were some limitations to MRgFUS disruption of the BBB in the brainstem in our study. In the rat, the depth of MRgFUS targeting is somewhat challenging due to the small size and shallow configuration of the cranial vault. As a result, the centre point of the MRgFUS target is set more posteriorly towards the cerebellum to minimize reflections of the ultrasound beam from the skull base. Such reflections can considerably increase the acoustic intensity and cause harm [46]. The use of a more posteriorly placed FUS target may help to explain the accumulation of some Evan's blue dye in the cerebellum relative to the brainstem in cross section. In mice, this also likely explains the increase in doxorubicin detected in the cerebellum in the "MRgFUS + μB" group although this was not a statistically significant increase. In addition, we used a single FUS transducer in our rodent model. The use of a single transducer limits the specificity of the targeted focal area resulting in an ellipsoid shaped region of coverage [47]. The geometry of the human brain permits the use of multiple transducers which improve the ability to achieve discrete in-depth focusing. The clinical transducer is also better able to reduce the distortion of the ultrasound wave from variations in thickness of the skull [48]. Nonetheless, we were able to demonstrate MR confirmation of BBB disruption in the rat brainstem following administration of Gadolinium using our technique. Evans Blue

distribution in brainstem cross sections also clearly depicts that despite the aforementioned limitations, diffuse dye uptake was seen throughout the brainstem at the level of the pons. It is anticipated that even greater specificity of targeting of the pons will be possible with the use of MRgFUS in patients with DIPG where such anatomical constraints of the skull base are not so problematic.

We also used cisplatin with the MRgFUS technique in our study to confirm that the delivery of a chemotherapeutic agent through the BBB and into the brainstem, did not cause harm. This was confirmed as rats in the "MRgFUS + μB + Cis" group did not demonstrate impaired function or tissue damage.

Cisplatin was chosen for use in our initial rat studies as it is a chemotherapy agent commonly used as part of combination chemotherapy regimens in the pediatric population. However, following its limited efficacy in our DIPG cell lines, doxorubicin was chosen for use in our mouse studies. In addition to its in vitro efficacy and poor BBB permeability, its pharmacokinetic profile has previously been studied in combination with MRgFUS mediated BBB disruption and the optimal delivery method to achieve high tissue penetrance whilst minimising toxicity has been determined [49].

Interestingly, in our study, both rat rotarod performance and grip strength were modestly improved after MRgFUS treatment of the brainstem. We attribute this improvement to enhanced performance by the rats from repeated measures as the same operator performed all measures pre- and post-procedure. This is a documented finding in the literature described as long-term improvement and is a more probable explanation than the μB or MRgFUS resulting in brain changes that would enhance their performance [50]. We used a single operator so as to reduce the likelihood of variations attributed to technique.

Monitoring of cardiorespiratory parameters was undertaken for several minutes following MRgFUS and there is the potential that delayed cardiorespiratory effects arose.

However, all of our rats reached the 14 day time point for histological analysis post treatment without any behavioural evidence of distress.

The μB dose used in our study was twice that of the maximum clinical dose. However, in clinical translation, more focal locations could be treated following a single bolus by scanning the ultrasound focus faster than is achievable with the small animal platform used in this study. Alternatively, a lower μB dose per injection could be used to allow more sonications within the allowable total dose [51]. Thus in practice, treatments could be performed without exceeding the maximum clinical dose.

Although we propose the use of MRgFUS as a repeatable therapy, we have not demonstrated the safety of repeated treatments in this study. However, repeated focused ultrasound treatment of the visual pathways has been previously performed in rhesus macaques and did not result in either histological damage, behavioural change or the ability of the animals to perform complex visual tasks [46]. Kovacs et al. however, have described sterile inflammation arising in the brain parenchyma of rodents treated with MRgFUS [52]. We attribute this to the group's use of a single, fixed ultrasound pressure as well as a significantly higher μB dose, with both factors having been shown to result in tissue injury [30]. In particular, our utilisation of a hydrophone receptor enables the detection of ultra and subharmonic emissions indicating stable microbubble cavitation and the automated selection of a sonication pressure previously validated to achieve consistent BBB opening without tissue damage [30]. Indeed, more recently, McMahon et al. have conducted a study directly comparing these parameters. They were able to demonstrate contrasting differences in the degree of inflammatory response and tissue damage consequent to the differing parameters [53].

Following our demonstration of the feasibility of MRgFUS BBB disruption in the rodent brainstem, we have successfully quantified the degree of enhanced drug uptake in the

region. The high doxorubicin concentration recorded in the brainstem at two hours is considerable given both the short plasma and tissue half-life of unencapsulated doxorubicin (5.3 minutes and between 9-23 minutes respectively) [54]. This enhanced drug uptake in the region of MRgFUS and doxorubicin treated tissue has been shown to persist at 24 hours in a supratentorial high grade tumour model [55]. Rather uniquely, MRgFUS enables focal BBB opening with our study demonstrating significantly enhanced doxorubicin uptake in the brainstem alone as compared to all other brain regions. Although we have demonstrated the ability to reach brainstem concentrations that exceed our in vitro IC50 concentration, we are aware that this may not confer a meaningful therapeutic response and this will be the subject of further work validating the use of MRgFUS in DIPG mouse models. We do however feel that the ability to achieve such a concentration confers significant promise in a disease process in which the BBB is a significant barrier to drug delivery.

In conclusion, in this study we have demonstrated the pre-clinical feasibility of brainstem BBB disruption using MRgFUS. We have also demonstrated the potential for increased and focal drug delivery to the brainstem. Future studies include the scaling up of this technique in larger animal systems in addition to testing the pre-clinical efficacy of selected chemotherapeutics in orthotopic patient-derived xenograft or genetically engineered models of DIPG. Now that the main molecular genetic drivers of DIPG are known [7-9,11-14] there is also a need for rational targeting of these tumours with highly specific pathway inhibitors. It is our hope that MRgFUS may play an important role in overcoming the BBB and providing a safe and reliable drug delivery strategy for the future treatment of DIPG.

Acknowledgements:

We thank Shawna Rideout-Gros and Viva Chan for help with animal care and preparation. We thank Kristina Mikloska and Sanjana Seerala for experimental assistance.

Funding:

This study was supported by grants from the Canadian Institutes of Health Research, Curing Kids Cancer Foundation, Brainchild, Meagan's Walk, the Laurie Berman, Rob Keyes and Wiley Funds for Brain Tumour Research, The Cure Starts Now, The DIPG Collaborative and the National Institutes of Health (R01- EB003268), as well as the Canada Research Chair Program. Saira Alli was supported by the Harry Morton Fellowship award from the Royal College of Surgeons of England.

References:

[1] G.I. Jallo, D. Freed, C. Roonprapunt, F. Epstein, Current management of brainstem gliomas, Annals of Neurosurgery, 2003.

[2] C.R. Freeman, G. Perilongo, Chemotherapy for brain stem gliomas, Childs Nerv Syst. 15 (1999) 545–553. doi:10.1007/s003810050542.

[3] S.S. Donaldson, Advances Toward an Understanding of Brainstem Gliomas, Journal of Clinical Oncology. 24 (2006) 1266–1272. doi:10.1200/JCO.2005.04.6599.

[4] A.L. Bredlau, D.N. Korones, Diffuse Intrinsic Pontine Gliomas: Treatments and Controversies, 1st ed., Elsevier Inc, 2014. doi:10.1016/B978-0-12-800249-0.00006-8.

[5] K.J. Cohen, N. Jabado, J. Grill, Diffuse intrinsic pontine gliomas—current management and new biologic insights. Is there a glimmer of hope? Neuro-Oncology. 19 (2017) 1025–1034. doi:10.1093/neuonc/nox021.

[6] K.A. Bradley, I.F. Pollack, J.M. Reid, P.C. Adamson, M.M. Ames, G. Vezina, et al., Motexafin gadolinium and involved field radiation therapy for intrinsic pontine glioma of childhood: a Children's Oncology Group phase I study, Neuro-Oncology. 10 (2008) 752–758. doi:10.1215/15228517-2008-043.

[7] G. Wu, A. Broniscer, T.A. McEachron, C. Lu, B.S. Paugh, J. Becksfort, et al., Somatic histone H3 alterations in pediatric diffuse intrinsic pontine gliomas and non-brainstem glioblastomas, Nat Genet. 44 (2012) 251–253. doi:10.1038/ng.1102.

[8] D.-A. Khuong-Quang, P. Buczkowicz, P. Rakopoulos, X.-Y. Liu, A.M. Fontebasso, E. Bouffet, et al., K27M mutation in histone H3.3 defines clinically and biologically distinct subgroups of pediatric diffuse intrinsic pontine gliomas, Acta Neuropathol. 124 (2012) 439–447. doi:10.1007/s00401-012-0998-0.

[9] J. Schwartzentruber, A. Korshunov, X.-Y. Liu, D.T.W. Jones, E. Pfaff, K. Jacob, et al., Driver mutations in histone H3.3 and chromatin remodelling genes in paediatric glioblastoma, Nature. (2012) 1–8. doi:10.1038/nature10833.

[10] V. Ramaswamy, M. Remke, M.D. Taylor, An epigenetic therapy for diffuse intrinsic pontine gliomas, Nature Publishing Group. 20 (2014) 1378–1379. doi:10.1038/nm.3769.

[11] K.R. Taylor, A. Mackay, N. Truffaux, Y.S. Butterfield, O. Morozova, C. Philippe, et al., Recurrent activating ACVR1 mutations in diffuse intrinsic pontine glioma, Nat Genet. 46 (2014) 457–461. doi:10.1038/ng.2925.

[12] P. Buczkowicz, U. Bartels, E. Bouffet, O. Becher, C. Hawkins, Histopathological spectrum of paediatric diffuse intrinsic pontine glioma: diagnostic and therapeutic implications, Acta Neuropathol. 128 (2014) 573–581. doi:10.1007/s00401-014-1319-6.

[13] G. Wu, A.K. Diaz, B.S. Paugh, S.L. Rankin, B. Ju, Y. Li, et al., The genomic landscape of diffuse intrinsic pontine glioma and pediatric non-brainstem high-grade glioma, Nat Genet. 46 (2014) 444–450. doi:10.1038/ng.2938.

[14] A.M. Fontebasso, S. Papillon-Cavanagh, J. Schwartzentruber, H. Nikbakht, N. Gerges, P.-O. Fiset, et al., Recurrent somatic mutations in ACVR1 in pediatric midline high-grade astrocytoma, Nat Genet. 46 (2014) 462–466. doi:10.1038/ng.2950.

[15] C.S. Grasso, Y. Tang, N. Truffaux, N.E. Berlow, L. Liu, M.-A. Debily, et al., Functionally defined therapeutic targets in diffuse intrinsic pontine glioma, Nat Med. 21 (2015) 555–559. doi:10.1038/nm.3855.

[16] A.B. Etame, R.J. Diaz, C.A. Smith, T.G. Mainprize, K. Hynynen, J.T. Rutka, Focused ultrasound disruption of the blood-brain barrier: a new frontier for therapeutic delivery in molecular neurooncology, Neurosurg Focus. 32 (2012) E3–17. doi:10.3171/2011.10.FOCUS11252.

[17] F. Marquet, Y.-S. Tung, T. Teichert, V.P. Ferrera, E.E. Konofagou, Noninvasive, Transient and Selective Blood-Brain Barrier Opening in Non-Human Primates In Vivo, PLoS ONE. 6 (2011) e22598–7. doi:10.1371/journal.pone.0022598.

[18] K. Hynynen, N. McDannold, N. Vykhodtseva, F.A. Jolesz, Noninvasive MR Imaging–guided Focal Opening of the Blood-Brain Barrier in Rabbits1, Radiology. 220 (2001) 640–646. doi:10.1148/radiol.2202001804.

[19] X. Shang, P. Wang, Y. Liu, Z. Zhang, Y. Xue, Mechanism of Low-Frequency Ultrasound in Opening Blood–Tumor Barrier by Tight Junction, J Mol Neurosci. 43 (2010) 364–369. doi:10.1007/s12031-010-9451-9.

[20] N. Sheikov, N. McDannold, F. Jolesz, Y.-Z. Zhang, K. Tam, K. Hynynen, Brain arterioles show more active vesicular transport of blood-borne tracer molecules than capillaries and venules after focused ultrasound-evoked opening of the blood-brain barrier, Ultrasound in Medicine & Biology. 32 (2006) 1399–1409. doi:10.1016/j.ultrasmedbio.2006.05.015.

[21] N. Sheikov, N. McDannold, S. Sharma, K. Hynynen, Effect of Focused Ultrasound Applied With an Ultrasound Contrast Agent on the Tight Junctional Integrity of the Brain Microvascular Endothelium, Ultrasound in Medicine & Biology. 34 (2008) 1093–1104. doi:10.1016/j.ultrasmedbio.2007.12.015.

[22] M.A. O'Reilly, O. Hough, K. Hynynen, Blood-Brain Barrier Closure Time After Controlled Ultrasound-Induced Opening Is Independent of Opening Volume, J Ultrasound Med. (2017) 1–9. doi:10.7863/ultra.16.02005.

[23] L.H. Treat, N. McDannold, Y. Zhang, N. Vykhodtseva, K. Hynynen, Improved Anti-Tumor Effect of Liposomal Doxorubicin After Targeted Blood-Brain Barrier

Disruption by MRI-Guided Focused Ultrasound in Rat Glioma, Ultrasound in Medicine & Biology. 38 (2012) 1716–1725. doi:10.1016/j.ultrasmedbio.2012.04.015.

[24] K.-C. Wei, P.-C. Chu, H.-Y.J. Wang, C.-Y. Huang, P.-Y. Chen, H.-C. Tsai, et al., Focused Ultrasound-Induced Blood–Brain Barrier Opening to Enhance Temozolomide Delivery for Glioblastoma Treatment: A Preclinical Study, PLoS ONE. 8 (2013) e58995–10. doi:10.1371/journal.pone.0058995.

[25] R. Alkins, A. Burgess, M. Ganguly, G. Francia, R. Kerbel, W.S. Wels, et al., Focused Ultrasound Delivers Targeted Immune Cells to Metastatic Brain Tumors, Cancer Research. 73 (2013) 1892–1899. doi:10.1158/0008-5472.CAN-12-2609.

[26] M. Kinoshita, N. McDannold, F.A. Jolesz, K. Hynynen, Noninvasive localized delivery of Herceptin to the mouse brain by MRI-guided focused ultrasound-induced blood-brain barrier disruption, Proc. Natl. Acad. Sci. U.S.a. 103 (2006) 11719–11723. doi:10.1073/pnas.0604318103.

[27] G.T. Clement, K. Hynynen, A non-invasive method for focusing ultrasound through the human skull, Phys Med Biol. 47 (2002) 1219–1236. doi:10.1088/0031-9155/45/12/314.

[28] R.J. Diaz, P.Z. McVeigh, M.A. O'Reilly, K. Burrell, M. Bebenek, C. Smith, et al., Focused ultrasound delivery of Raman nanoparticles across the blood-brain barrier: Potential for targeting experimental brain tumors, Nanomedicine: Nanotechnology, Biology, and Medicine. 10 (2014) e1075–e1087. doi:10.1016/j.nano.2013.12.006.

[29] M.A. O'Reilly, K. Hynynen, A PVDF Receiver for Ultrasound Monitoring of Transcranial Focused Ultrasound Therapy, IEEE Trans. Biomed. Eng. 57 (2011) 2286–2294. doi:10.1109/TBME.2010.2050483.

[30] M.A. O'Reilly, K. Hynynen, Blood-Brain Barrier: Real-time Feedback-controlled Focused Ultrasound Disruption by Using an Acoustic Emissions–based Controller, Radiology. 263 (2012) 96–106. doi:10.1148/radiol.11111417.

[31] S.-K. Wu, P.-C. Chu, W.-Y. Chai, S.-T. Kang, C.-H. Tsai, C.-H. Fan, et al., Characterization of Different Microbubbles in Assisting Focused Ultrasound-Induced Blood-Brain Barrier Opening, Scientific Reports. (2017) 1–11. doi:10.1038/srep46689.

[32] S.J.E. Veringa, D. Biesmans, D.G. van Vuurden, M.H.A. Jansen, L.E. Wedekind, I. Horsman, et al., In Vitro Drug Response and Efflux Transporters Associated with Drug Resistance in Pediatric High Grade Glioma and Diffuse Intrinsic Pontine Glioma, PLoS ONE. 8 (2013) e61512–10. doi:10.1371/journal.pone.0061512.

[33] G. Wei, S. Xiao, D. Si, C. Liu, Improved HPLC method for doxorubicin quantification in rat plasma to study the pharmacokinetics of micelle-encapsulated and liposome-encapsulated doxorubicin formulations, Biomed. Chromatogr. 22 (2008) 1252–1258. doi:10.1002/bmc.1054.

[34] R.D. Arnold, J.E. Slack, R.S.J.O.C. B, 2004, Quantification of Doxorubicin and metabolites in rat plasma and small volume tissue samples by liquid chromatography/electrospray tandem mass spectroscopy, Elsevier. 808 (2004) 141–152. doi:10.1016/j.jchromb.2004.04.030.

[35] M.A. O'Reilly, A. Muller, K. Hynynen, Ultrasound Insertion Loss of Rat Parietal Bone Appears to Be Proportional to Animal Mass at Submegahertz Frequencies, Ultrasound in Medicine & Biology. 37 (2011) 1930–1937. doi:10.1016/j.ultrasmedbio.2011.08.001.

[36] N. McDannold, N. Vykhodtseva, S. Raymond, F.A. Jolesz, K. Hynynen, MRI-guided targeted blood-brain barrier disruption with focused ultrasound: histological findings in rabbits, Ultrasound in Medicine & Biology. 31 (2005) 1527–1537. doi:10.1016/j.ultrasmedbio.2005.07.010.

[37] H.W. Bothe, W. Bodsch, K.A. Hossmann, Relationship between specific gravity, water content, and serum protein extravasation in various types of vasogenic brain edema, Acta Neuropathol. 64 (1984) 37–42.

[38] C. Rousselle, P. Clair, J.M. Lefauconnier, M. Kaczorek, J.M. Scherrmann, J. Temsamani, New advances in the transport of doxorubicin through the blood-brain barrier by a peptide vector-mediated strategy, Mol. Pharmacol. 57 (2000) 679–686.

[39] T. Ohnishi, I. Tamai, K. Sakanaka, A. Sakata, T. Yamashima, J. Yamashita, et al., In vivo and in vitro evidence for ATP-dependency of P-glycoprotein-mediated efflux of doxorubicin at the blood-brain barrier, Biochem. Pharmacol. 49 (1995) 1541–1544.

[40] M.I. Vanan, D.D. Eisenstat, DIPG in Children – What Can We Learn from the Past? Front. Oncol. 5 (2015) v1–17. doi:10.3389/fonc.2015.00237.

[41] N. Lipsman, T.G. Mainprize, M.L. Schwartz, K. Hynynen, A.M. Lozano, Intracranial Applications of Magnetic Resonance-guided Focused Ultrasound, Neurotherapeutics. 11 (2014) 593–605. doi:10.1007/s13311-014-0281-2.

[42] M.M. Souweidane, K. Kramer, N. Pandit-Taskar, P. Zanzonico, Z. Zhou, M. Donzelli, et al., A phase I study of convection enhanced delivery (CED) of 124I-8H9 radio-labeled monoclonal antibody in children with diffuse intrinsic pontine glioma (DIPG), Journal of Clinical Oncology. 35 (2017) 2010–2010. doi:10.1200/JCO.2017.35.15_suppl.2010.

[43] R.C.E. Anderson, B. Kennedy, C.L. Yanes, J. Garvin, M. Needle, P. Canoll, et al., Convection-enhanced delivery of topotecan into diffuse intrinsic brainstem tumors in children, J Neurosurg Pediatr. 11 (2013) 289–295. doi:10.3171/2012.10.PEDS12142.

[44] O. Lewis, M. Woolley, D. Johnson, A. Rosser, N.U. Barua, A.S. Bienemann, et al., Chronic, intermittent convection-enhanced delivery devices, Journal of Neuroscience Methods. 259 (2016) 47–56. doi:10.1016/j.jneumeth.2015.11.008.

[45] J.S. Kroin, R.D. Penn, Intracerebral chemotherapy: chronic microinfusion of cisplatin, Neurosurgery. 10 (1982) 349–354.

[46] N. McDannold, C.D. Arvanitis, N. Vykhodtseva, M.S. Livingstone, Temporary disruption of the blood-brain barrier by use of ultrasound and microbubbles: safety and efficacy evaluation in rhesus macaques, Cancer Research. 72 (2012) 3652–3663. doi:10.1158/0008-5472.CAN-12-0128.

[47] F.A. Jolesz, K.H. Hynynen, MRI-Guided Focused Ultrasound Surgery, CRC Press, 2007.

[48] A. Burgess, K. Shah, O. Hough, K. Hynynen, Focused ultrasound-mediated drug delivery through the blood–brain barrier, Expert Review of Neurotherapeutics. 15 (2015) 477–491. doi:10.1586/14737175.2015.1028369.

[49] T. Nhan, A. Burgess, L. Lilge, K. Hynynen, Modeling localized delivery of Doxorubicin to the brain following focused ultrasound enhanced blood-brain barrier permeability, Phys Med Biol. 59 (2014) 5987–6004. doi:10.1088/0031-9155/59/20/5987.

[50] M. Buitrago, Short and long-term motor skill learning in an accelerated rotarod training paradigm, Neurobiology of Learning and Memory. 81 (2004) 211–216. doi:10.1016/j.nlm.2004.01.001.

[51] Y. Huang, R. Alkins, M.L. Schwartz, K. Hynynen, Opening the Blood-Brain Barrier with MR Imaging–guided Focused Ultrasound: Preclinical Testing on a Trans–Human Skull Porcine Model, Radiology. 282 (2017) 123–130. doi:10.1148/radiol.2016152154.

[52] Z.I. Kovacs, S. Kim, N. Jikaria, F. Qureshi, B. Milo, B.K. Lewis, et al., Disrupting the blood–brain barrier by focused ultrasound induces sterile inflammation, Proc. Natl. Acad. Sci. U.S.a. 114 (2017) E75–E84. doi:10.1073/pnas.1614777114.

[53] D. McMahon, K. Hynynen, Acute Inflammatory Response Following Increased Blood-Brain Barrier Permeability Induced by Focused Ultrasound is Dependent on Microbubble Dose, Theranostics. 7 (2017) 3989–4000. doi:10.7150/thno.21630.

[54] A. Rahman, D. Carmichael, M. Harris, J.K. Roh, Comparative Pharmacokinetics of Free Doxorubicin and Doxorubicin Entrapped in Cardiolipin Liposomes, Cancer Research. 46 (1986) 2295–2299.

[55] J. Park, M. Aryal, N. Vykhodtseva, Y.-Z. Zhang, N. McDannold, Evaluation of permeability, doxorubicin delivery, and drug retention in a rat brain tumor model after ultrasound-induced blood-tumor barrier disruption, Journal of Controlled Release. 250 (2017) 77–85. doi:10.1016/j.jconrel.2016.10.011.

Figure legends:

Figure 1: A. Brainstem sonication schema used in Sprague Dawley rats. MRgFUS was delivered to a region comprising of a four-point overlapping grid in each half of the pons. **B. Contrast enhanced T1-weighted MR imaging of BBB opening in rats.** Axial and sagittal views of MR imaging performed pre- and post-FUS delivery to the rodent brainstem. Rats who were treated with microbubbles only (μB) or MRgFUS only did not demonstrate contrast enhancement within the brainstem on post procedure imaging. Animals that received MRgFUS and microbubbles (MRgFUS + μB) did show brainstem enhancement, thereby confirming BBB opening (circles and arrows). The administration of the chemotherapy agent cisplatin (1.5 mg/kg) in addition to the focused ultrasound and microbubbles (MRgFUS + μB + Cis) did not affect the ability to achieve BBB opening and contrast enhancement within the brainstem was still seen (circles and arrows).

Figure 2: Evans Blue staining of rodent brainstem confirming BBB opening. Rats were treated with either microbubbles only (μB), MRgFUS or both (MRgFUS + μB). Control "Evans Blue" rats received no intervention. Following treatment, 4% Evans Blue was administered intravenously. Animals were then perfused (4% PFA) and brainstem specimens were extracted, sectioned and imaged. Blue staining was observed on the anterior aspect of the brainstem and on cross-section of animals in the (MRgFUS + μB) group only, thereby confirming BBB permeability in the region. This was not true for the "μB", "MRgFUS" and "Evans Blue" treated animals.

Figure 3: Physiological monitoring of heart and respiratory rate. The MouseOx rodent monitoring system was used to monitor the heart rate (in red) and respiratory rate (in blue) of rats during focused ultrasound delivery to the brainstem. Rats were randomised to one of four

treatment groups; **A)** microbubbles only (μB), **B)** focused ultrasound only (MRgFUS), **C)** focused ultrasound and microbubbles (MRgFUS + μB) with a final group consisting of the latter in conjunction with intravenous Cisplatin delivery (MRgFUS + μB + Cis) **(D)**. Monitoring was initiated four minutes prior to sonication and continued for four minutes after. The brainstem was treated in two halves - right and left (pink bars) with re-administration of microbubbles between treatments due to their short half-life. No significant fluctuations or abrupt cessation of either parameter was noted during treatment indicating preservation of the brainstem cardiorespiratory control centres.

Figure 4: Comparison of mean heart rate and respiratory rate recordings of rats before, during and after the specified procedures. The MouseOx rodent monitoring system was used to monitor the heart rate and respiratory rate of rats during focused ultrasound delivery to the brainstem. Rats were randomised to one of four treatment groups; **A)** microbubbles only (μB), **B)** focused ultrasound only (MRgFUS), **C)** focused ultrasound and microbubbles (MRgFUS + μB) with a final group consisting of the latter in conjunction with intravenous Cisplatin delivery (MRgFUS + μB + Cis) **(D)**. Monitoring was initiated four minutes "before" the sonication (filled shapes) continued "during" sonication (half-filled shapes) and continued for four minutes "after" completion of the sonication (empty shapes). The mean recording for each rat within each treatment group is plotted. The mean and standard deviation of each group is represented by horizontal lines. No statistically significant difference in heart and respiratory rate were noted "during" and "after" any of the interventions when compared to baseline "before" recordings (Two way multivariate mixed model ANOVA, $p>0.05$).

Figure 5: Comparison of rotarod and grip strength performance pre-and post-procedure. Rats were tested one week pre (filled shapes) and one week post (empty shapes) intervention with either microbubbles alone (μB), focused ultrasound alone (MRgFUS), focused ultrasound and microbubbles (MRgFUS + μB) or focused ultrasound with microbubbles and cisplatin (MRgFUS + μB + Cis). No difference in rotarod performance **(A)** or grip strength **(B)** was identified when comparing treatment groups (2 way mixed MANOVA with Tukey's post hoc test, * $p<0.05$ for rotarod, ** $p<0.001$ for grip strength). A significant improvement in performance was noted in both rotarod and grip strength pre-and post-procedure.

Figure 6: Hematoxylin and eosin (H&E) staining of brainstem sections. Following focused ultrasound delivery, brainstem samples were retrieved at early (4 hours) and late (14 days) post intervention. **(A)** Schematic demonstrating that three regions of the brainstem were sectioned and analysed. **(B)** Treated samples ("MRgFUS + μB") were compared to "untreated" controls. No evidence of tissue damage in the form of haemorrhage or vacuolation was seen at either the early or late time points.

Figure 7: Quantification of Caspase 3 and NeuN staining of brainstem samples. Histological analysis of brainstem samples was conducted at early (4 hours) and late (14 day) time points. Three levels of the brainstem were assessed for **(A)** Caspase 3 staining as a marker of apoptosis and **(B)** NeuN staining of neuronal nuclei for quantification. No significant difference in the percentage area of caspase 3 staining or neuronal number was identified across all groups at either time point (Three-way MANOVA with Tukey's post hoc test).

Figure 8: DIPG Drug Screen. A drug screen consisting of eight conventional chemotherapeutic agents was conducted in three patient derived DIPG cell lines (SU-DIPG IV,

SU-DIPG XIII and SU-DIPG XVII). **(A)** Dose ranges for each drug tested are outlined and were obtained from previously published IC_{50} data in the literature. **(B)** A heat map was generated from twelve-point dose escalation curves to demonstrate cell viability at escalating drug concentrations (left to right). **(C)** Dose escalation curves for Doxorubicin and Temozolamide are highlighted to demonstrate the differing efficacy of the two agents in our cell lines.

Figure 9: Brain Doxorubicin Distribution. NOD/SCID/GAMMA mice were injected with 5mg/kg intravenous Doxorubicin with either no intervention, microbubbles alone (μB), focused ultrasound alone (MRgFUS) or both microbubbles and focused ultrasound (MRgFUS + μB). Focused ultrasound, when used, was targeted at the brainstem specifically. Greatest Doxorubicin uptake was seen in the brainstem of the MRgFUS + μB treated group as compared to all other groups and brain regions (two- way mixed ANOVA, ** $p < 0.01$, *** $p < 0.001$).

Supplementary Figures:

Supplementary Figure 1: Caspase 3 stained sections at early and late time points. Following treatment with focused ultrasound and intravenously administered microbubbles, rodents were perfused and brainstems retrieved at 4-hour **(MRgFUS + μB EARLY)** and 14 day (**MRgFUS + μB LATE)** time points. Brainstems were sectioned at three levels and stained for Caspase 3 activity as a marker of apoptosis. Sections were compared to Caspase 3 stained sections of untreated controls **(Untreated).** No difference in the degree of Caspase 3 staining was noted.

Supplementary Figure 2: NeuN stained sections at early and late time points. Following treatment with focused ultrasound and intravenously administered microbubbles, rodents were perfused and brainstems retrieved at 4-hour **(MRgFUS + μB EARLY)** and 14 day **(MRgFUS + μB LATE)** time points. Brainstems were sectioned at three levels and stained for NeuN to

quantify neuronal number. Sections were compared to Caspase 3 stained sections of untreated controls **(Untreated).** No difference in the number or morphology of neurons was identified.

Supplementary Figure 3: (**A) Brainstem sonication schema used in NSG Mice.** MRgFUS was delivered to a region comprising of a four-point overlapping grid in the centre of the pons. **B. Contrast enhanced T1-weighted MR imaging of BBB opening in mice.** Axial and sagittal views of MR imaging performed pre- and post-FUS delivery to the murine brainstem. Mice who received "no intervention" or were treated with microbubbles only (μB) or MRgFUS only (MRgFUS) did not demonstrate contrast enhancement within the brainstem on post procedure imaging. Animals that received MRgFUS and microbubbles (MRgFUS + μB) did show brainstem enhancement, thereby confirming BBB opening (circle and arrow).

SUPPLEMENTARY DATA (at reviewers request):

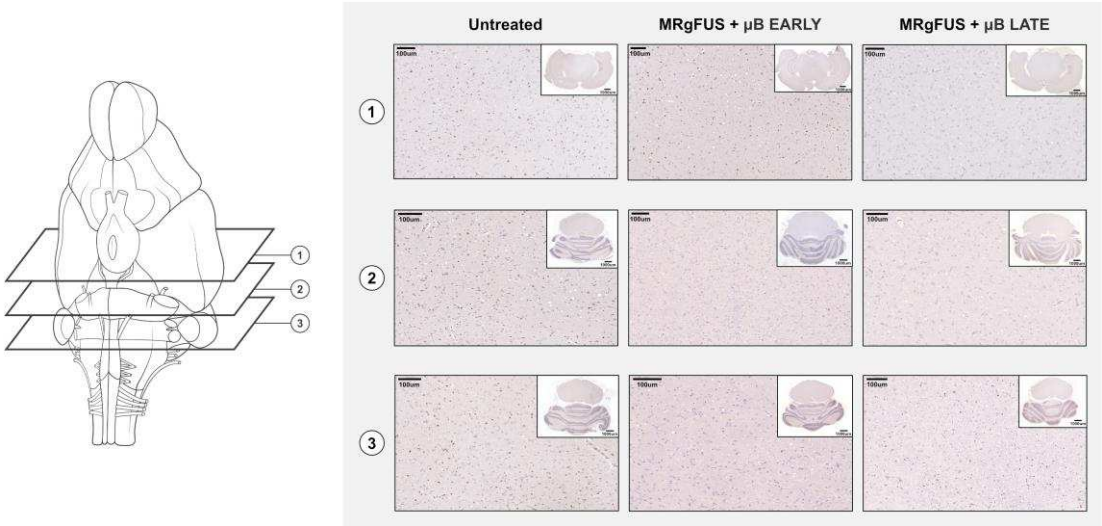

Supplementary Figure 1: Caspase 3 stained sections at early and late time points. Following treatment with focused ultrasound and intravenously administered microbubbles, rodents were perfused and brainstems retrieved at 4-hour **(MRgFUS + µB EARLY)** and 14 day (**MRgFUS + µB LATE)** time points. Brainstems were sectioned at three levels and stained for Caspase 3 activity as a marker of apoptosis. Sections were compared to Caspase 3 stained sections of untreated controls **(Untreated).** No difference in the degree of Caspase 3 staining was noted.

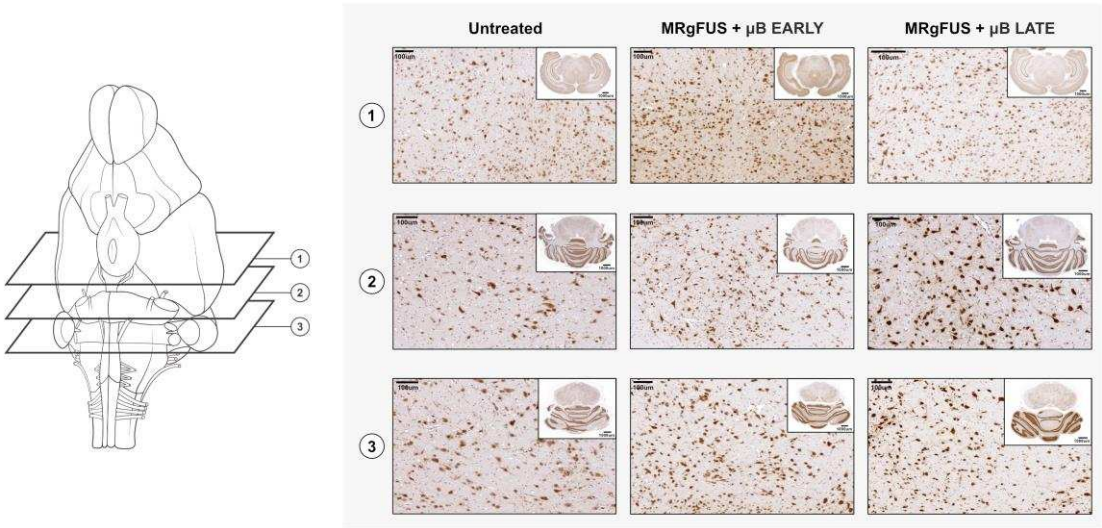

Supplementary Figure 2: NeuN stained sections at early and late time points. Following treatment with focused ultrasound and intravenously administered microbubbles, rodents were perfused and brainstems retrieved at 4-hour **(MRgFUS + µB EARLY)** and 14 day **(MRgFUS + µB LATE)** time points. Brainstems were sectioned at three levels and stained for NeuN to quantify neuronal number. Sections were compared to Caspase 3 stained sections of untreated controls **(Untreated).** No difference in the number or morphology of neurons was identified.

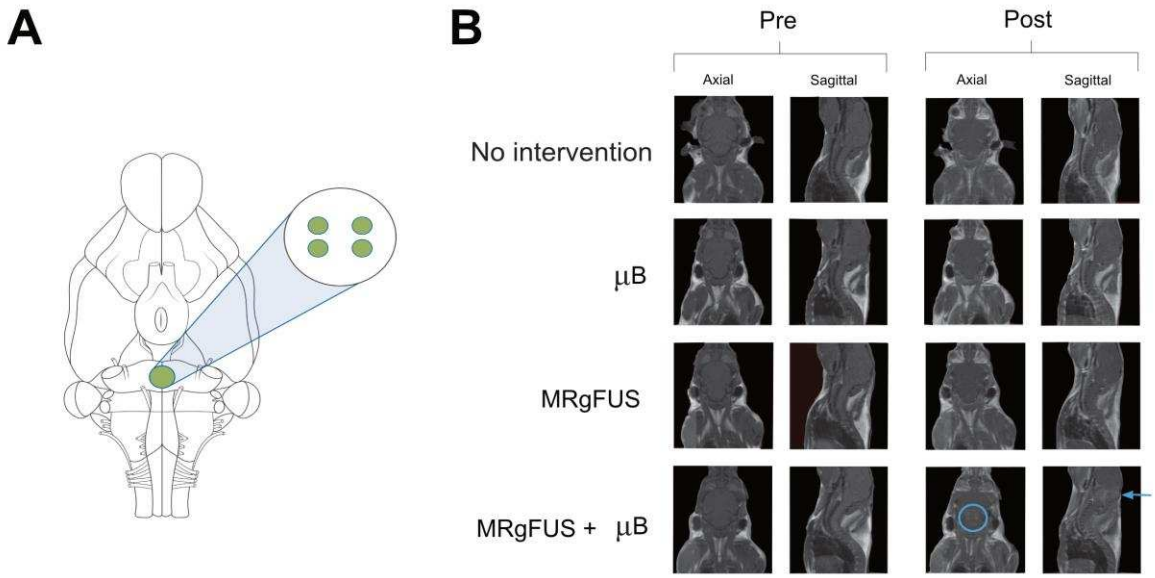

Supplementary Figure 3: (A) Brainstem sonication schema used in NSG Mice. MRgFUS was delivered to a region comprising of a four-point overlapping grid in the centre of the pons. **B. Contrast enhanced T1-weighted MR imaging of BBB opening in mice.** Axial and sagittal views of MR imaging performed pre- and post-FUS delivery to the murine brainstem. Mice who received "no intervention" or were treated with microbubbles only (μB) or MRgFUS only (MRgFUS) did not demonstrate contrast enhancement within the brainstem on post procedure imaging. Animals that received MRgFUS and microbubbles (MRgFUS + μB) did show brainstem enhancement, thereby confirming BBB opening (circle and arrow).

Supplementary Figure 4: Evans Blue staining of rodent brainstem confirming BBB opening (all rats). Rats were treated with either microbubbles only (μB), MRgFUS or both (MRgFUS + μB). Control rats received no intervention. Following treatment, 4% Evans Blue was administered intravenously. Animals were then perfused (4% PFA) and brainstem specimens were extracted, sectioned and imaged. Blue staining was observed on the anterior aspect of the brainstem and on cross-section of animals in the (MRgFUS + μB) group only, thereby confirming BBB permeability in the region. This was not true for the "μB", "MRgFUS" and "control" treated animals.

Please NB: Due to the large file size, this figure could not be embedded into this word document and has been uploaded to the submission website separately.